R-Matrix Evaluation of ^{16}O Neutron Cross Sections up to 6.3 MeV

R. O. Sayer*, L. C. Leal, N. M. Larson, R. R. Spencer, and R. Q. Wright

Oak Ridge National Laboratory, Oak Ridge, Tennessee 37831, USA

We have evaluated ^{16}O neutron cross sections in the resolved resonance region with the multilevel Reich-Moore code SAMMY. Resonance parameters were determined by a consistent analysis, including both Doppler and resolution broadening effects. To properly treat the α particle exit channel, an algorithm to calculate charged particle penetrabilities and shifts was incorporated into SAMMY.

KEYWORDS: resonance parameter evaluation, oxygen 16, neutron cross sections, alpha particle exit channel

I. Introduction

Over the years the nuclear community has developed a collection of evaluated nuclear data for applications in thermal, fast reactor, and fusion systems. In contrast to these systems, typical neutron spectra in criticality safety applications peak in the epithermal energy range. Because nuclear data play a major role in the calculation of criticality safety margins, a thorough examination of the behavior of present nuclear data evaluations in criticality safety calculations is needed. For oxygen, the existing ENDF/B-VI.5 evaluation is expressed in terms of point-wise cross sections derived from the analysis of G. Hale.[1)] Unfortunately such an evaluation is not directly useful for resonance analysis of data from samples in which oxygen is combined with other elements; for that purpose, resonance parameters are needed. In this paper we describe a resonance parameter evaluation of ^{16}O neutron cross sections in the resolved resonance region with the multilevel Reich-Moore R-matrix formalism using the code SAMMY.[2)] A preliminary report of this work has been given previously.[3)]

II. Cross Section and Differential Elastic Data

A search of standard nuclear databases and the open literature led to selection of total, reaction, and angle differential elastic cross section data sets for analysis; see **Tables 1** and **2**.

Table 1 Cross Section Data Sets for ^{16}O Evaluation

Authors	Facility	Energy Range (MeV)	Atoms/barn
Johnson, et al.[4)]	ORELA	0.2 - 6.3	0.183
Cierjacks, et al.[5)]	KFK cyclotron	3.14 - 6.3	1.201
Larson, et al.[6)]	ORELA	2.0 - 6.3	0.549
Fowler, et al.[7)]	ORNL VDG	0.6 - 6.3	0.488
Johnson, et al.[8)]	ORELA	2.25 - 2.49	6.700
Ohkubo[9)]	Linac	0.01 - 0.9	
Bair, Haas[10)]	ORNL VDG	3.2 - 6.3	
Drotleff, et al.[11)]	Stuttgart	2.87 - 3.48	

In the energy range of overlap, 0.6 - 4.3 MeV, the σ_{total} values for Refs. 4, 6, and 7 agree, but the Cierjacks data[5)] are 3.5% lower. The Cierjacks data were normalized to the ORELA data[4)] by integrating between 3.45 and 3.72 MeV. A neutron energy transformation was used to align the ORELA peak energies with the higher resolution Cierjacks values.

* Corresponding author, Tel. +1-865-574-4755
E-mail: sayerro@ornl.gov

The ^{16}O$(n,\alpha)^{13}$C channel opens at a laboratory neutron energy E_n = 2.36 MeV and contributes about 9% to σ_{total} at E_n = 4.18 MeV and about 25% at 5.07 MeV. Therefore, $\sigma_{n,\alpha}$ values deduced by reciprocity from ^{13}C$(\alpha,n)^{16}$O measurements by Bair and Haas[10)] and Drotleff, et al.[11)] were fit to obtain Γ_α values for several resonances. The Bair-Haas data exhibit good α energy resolution of 2 to 5 keV over the energy range of interest for this evaluation. Energy transformations were applied to align narrow resonances with the more precise Cierjacks energies.

Table 2 Angular Distribution Data Sets for ^{16}O Evaluation

Authors	Facility	Energy Range (MeV)	Θ_{CM} (deg)
Okazaki[12)]	Wisconsin	0.410 - 0.493	46 - 133
Fowler, Cohn[13)]	ORNL VDG	0.73 - 2.15	32 - 138
Phillips[14)]	LANL	3.0 - 6.0	22 - 152
Martin, Zucker[15)]	BNL	1.51 - 2.25	21 - 166
Hunzinger, Huber[16)]	Basel CW	2.00 - 4.11	41 - 147
Lister, Sayres[17)]	Columbia VDG	3.1 - 4.7	Leg. Coef.
Johnson, Fowler[18)]	ORNL VDG	3.266 - 4.200	20 - 147
Fowler, Johnson[19)]	ORNL VDG	1.833 - 3.441	20 - 146
Kinney, Perey[20)]	ORNL VDG	4.34 - 6.44	16 - 139
Drigo, et al.[21)]	Lignaro VDG	2.56 - 2.76	26 - 156

III. Resonance Analysis and Results

In order to give a proper treatment for charged particles in an exit channel, an algorithm[3)] to calculate charged particle penetrabilities (CPP) and shifts was incorporated in SAMMY. A slightly modified version of the routine COULFG of Barnett[22)] is used to compute Coulomb wave functions and derivatives. Routines based on the CPP algorithm have been integrated into a prototype modification of the NJOY[23)] code and will be incorporated in the AMPX[24)] code.

Resonance parameters were determined by a consistent analysis incorporating both Doppler and resolution broadening effects. Total and reaction data sets were analyzed sequentially so that each fit was connected to the previous fit by the SAMMY parameter covariance matrix, thereby yielding energies and widths for 37 resonances in the range $0 < E_n < 6.3$ MeV. Two negative-energy resonances were included to account for bound levels and 13 high-energy resonances were included to account for the effect of resonances above 6.3 MeV. Partial waves $s_{1/2}$ through $g_{9/2}$ were included in the analysis. The neutron channel radius, a_n , α channel radius,

a_α , and the $\sigma_{n,\alpha}$ normalization factor, $F_{n\alpha}$, were varied; final values were a_n = 3.80 fm, a_α = 6.7 fm, and $F_{n\alpha}$ = 1.00.

Figure 1 presents a global view of the final SAMMY fits to the total cross section data of Refs. 4–9. The (n,α) cross sections obtained by reciprocity from the (α,n) data of Ref. 10 and Ref. 11 are compared with the SAMMY fits in **Fig. 2**.

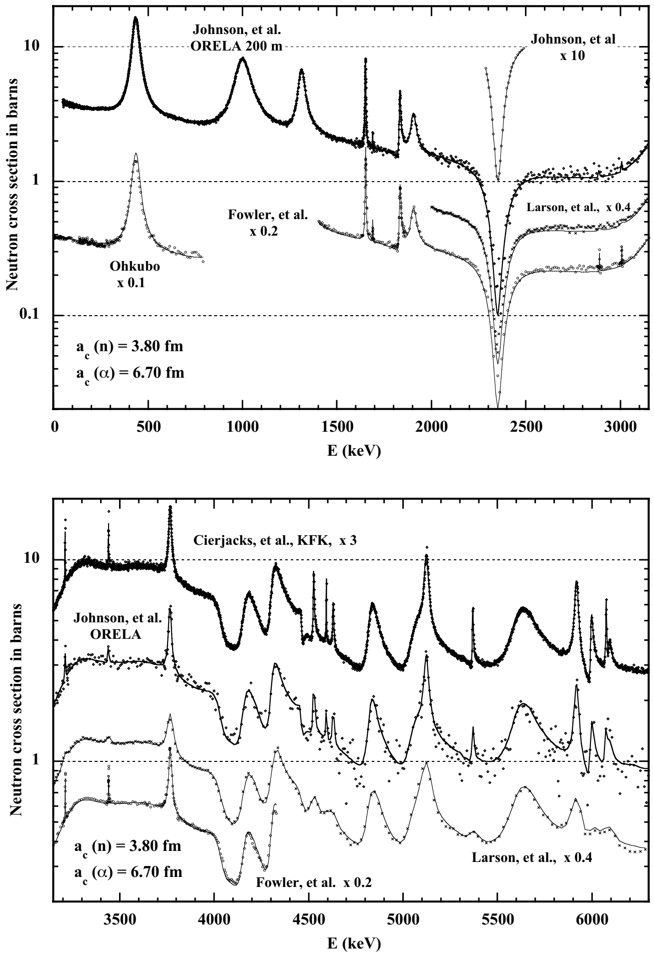

Fig. 1 Comparison of SAMMY predictions to ^{16}O σ_{total} data.[4–9] Data and predictions have been scaled for visual separation.

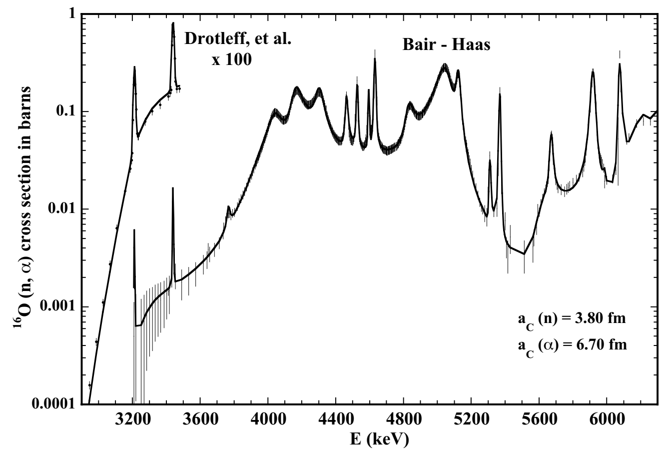

Fig. 2 Comparison of SAMMY predictions to $\sigma_{n,\alpha}$ data deduced by reciprocity from ^{13}C$(\alpha,n)^{16}$O data of Bair and Haas[10] and Drotleff et al.[11]

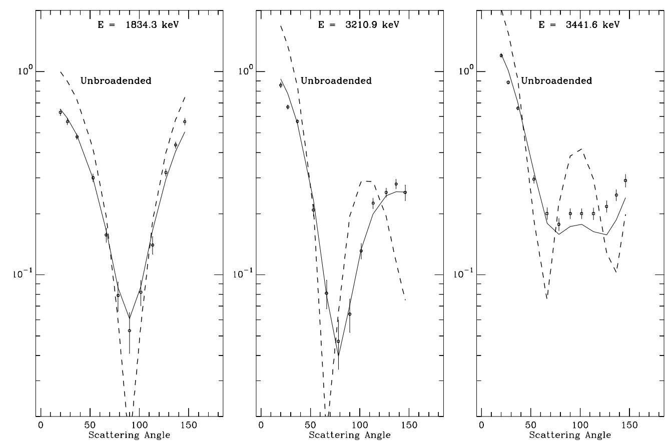

Fig. 3 Broadened (solid) and unbroadened (dashed) SAMMY predictions for $d\sigma/d\Omega$ data (points) of Fowler and Johnson.[19]

A rather large α channel radius, 6.7 fm, was required in order to fit the (n,α) data since the 3291 keV $d_{3/2}$ resonance (Γ_n = 340 keV, Γ_α = 0.17 keV) introduces a significant background for $E_n > 4.5$ MeV. This is due to the exponential increase of the Coulomb penetrability, and hence Γ_α , with E_n.

Spin-parity assignments were based on fits to σ_{total} and $\sigma_{n,\alpha}$ data and on comparison of predicted and experimental $d\sigma/d\Omega$ values. Where fits were inconsistent with the data, several J^π values were tried to improve the fits. Theoretical $d\sigma/d\Omega$ values were energy-broadened by the appropriate amount before comparison with the data. An example of the effect of energy broadening is given in **Fig. 3** for the data of Fowler and Johnson[19] for the 1834 keV $d_{3/2}$ resonance (ΔE = 13 keV, Γ = 7.8 keV), the 3212 keV $f_{5/2}$ resonance, and the 3442 keV $f_{5/2}$ resonance. The finite angular size of detectors was also taken into account in the SAMMY calculations.

Examples of $d\sigma/d\Omega$ data[18] are compared with SAMMY predictions in **Fig. 4**. Legendre coefficients given by Lister and Sayres[17] are compared with predicted values in **Fig. 5**.

When uncertainties are taken into account, predicted and experimental quantities are in satisfactory agreement.

Caro[25] has reported an evaluation of ^{16}O using a resonance plus potential well model which, unfortunately, does not provide a Reich-Moore resonance parameter representation. For the four non-resonant energies given by Caro (1.50, 1.75, 2.56, and 2.76 MeV), the differences between our predicted $d\sigma/d\Omega$ values and those of Caro are much smaller than the experimental uncertainties.

The ^{17}O level excitation energy E_x, resonance energy E_R, neutron width Γ_n, α width Γ_α, and J^π value are listed in **Table 3** for resonances included in the present evaluation. The resonance energies E_R correspond to the eigenenergies determined by the Reich-Moore analysis with SAMMY with boundary conditions chosen so that the level shifts are zero.

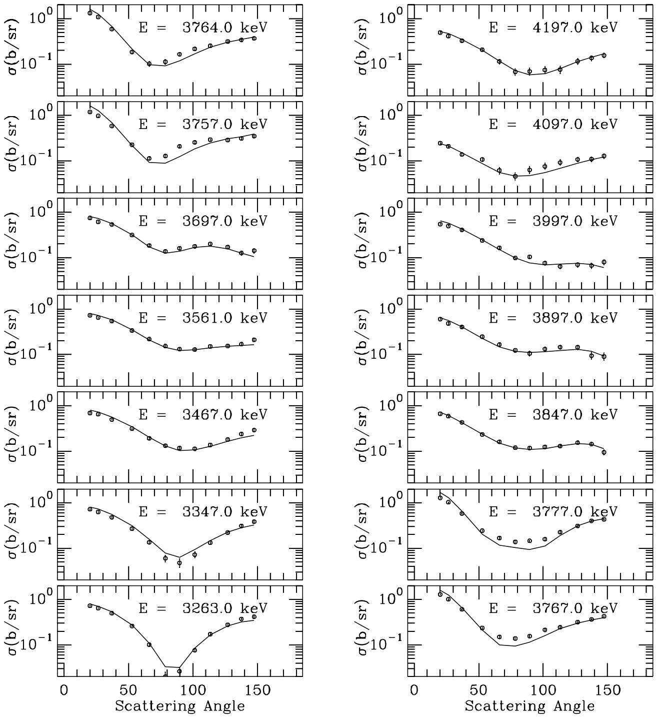

Fig. 4 Comparison of SAMMY predictions to selected differential elastic data of Johnson and Fowler.[18)]

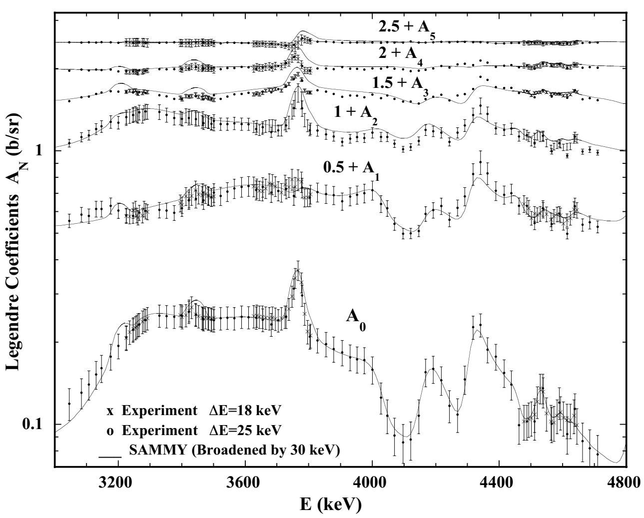

Fig. 5 Comparison of SAMMY predictions to Legendre coefficients of Lister and Sayres.[17)]

Table 3 Energies and Widths for Resonances in ^{16}O (n,X)

J^π	$E_x(^{17}$O) (keV)	E_R (keV)	Γ_n (keV)	Γ_α * (keV)
$3/2^-$	4551.9 ± 1.5	434.31	44.4 ± 1.5	
$3/2^+$	5084.2 ± 2.5	1000.22	100 ± 5	
$3/2^-$	5375.1 ± 2.0	1309.38	43.4 ± 1.7	
$7/2^-$	5696.7 ± 2.0	1651.38	4.10 ± 0.40	
$(5/2^-)$	5732.3 ± 1.9	1689.10	0.27 ± 0.05	
$3/2^+$	5868.7 ± 2.0	1834.09	7.79 ± 0.70	
$1/2^-$	5932.0 ± 2.3	1901.44	33.5 ± 2.5	
$1/2^+$	6380.2 ± 3.3	2377.88	162 ± 5	
$(5/2^+)$	6860.7 ± 2.0	2888.70	0.22 ± 0.08	
$(7/2^-)$	6971.9 ± 2.0	3006.90	0.16 ± 0.04	
$5/2^-$	7164.6 ± 0.4	3211.76	1.50 ± 0.15	0.009 ± 0.003
$3/2^+$	7239.1 ± 8.0	3291.01	340 ± 30	0.17 ± 0.03
$5/2^+$	7378.2 ± 0.4	3438.80	0.60 ± 0.20	0.020 ± 0.007
$5/2^-$	7380.8 ± 0.4	3441.55	1.30 ± 0.25	0.007 ± 0.005
$3/2^-$	7446.9 ±20.0	3511.91	660 ± 60	≈ 0.03
$7/2^-$	7686.9 ± 0.4	3767.00	18.5 ± 1.2	0.026 ± 0.008
$1/2^-$	7896.3 ± 6.0	3989.64	276 ± 25	19.0 ± 3.0
$1/2^+$	7963.3 ± 2.2	4060.82	106 ± 10	5.2 ± 1.5
$3/2^+$	8075.4 ± 2.1	4180.04	92.4 ± 6.0	9.8 ± 1.8
$3/2^-$	8190.9 ± 2.5	4302.79	54.3 ± 6.0	5.8 ± 1.0
$1/2^-$	8199.3 ± 4.5	4311.70	43.5 ± 9.0	- 0.4 ± 0.3
$1/2^+$	8345.7 ± 0.6	4467.36	16.9 ± 2.5	3.7 ± 0.7
$5/2^+$	8402.2 ± 0.2	4527.36	4.99 ± 0.30	0.86 ± 0.20
$7/2^+$	8465.6 ± 0.2	4594.83	1.39 ± 0.14	0.44 ± 0.10
$5/2^-$	8499.8 ± 0.3	4631.21	3.20 ± 0.20	3.9 ± 0.4
$3/2^-$	8677.7 ± 1.5	4820.33	58.4 ± 3.5	2.7 ± 0.5
$3/2^+$	8909.1 ± 4.0	5066.30	94.5 ± 12.0	- 34.4 ± 6.0
$7/2^-$	8963.2 ± 0.5	5123.74	23.4 ± 2.2	2.8 ± 0.5
$(1/2^-)$	9139.3 ± 6.0	5311.00	≈ 0.5	≈ 4.0
$5/2^+$	9194.1 ± 0.4	5369.27	2.78 ± 0.18	1.25 ± 0.30
$3/2^-$	9387.5 ±14.0	5574.84	191 ± 14	0.42 ± 0.15
$5/2^-$	9479.5 ± 4.1	5672.62	0.6 ± 0.3	15.6 ± 3.0
$7/2^+$	9710.9 ± 0.5	5918.63	20.5 ± 1.0	4.2 ± 0.6
$3/2^-$ a	9781.1 ± 0.5	5993.29	14.8 ± 1.2	≈ - 0.2
$9/2^+$ b	9859.1 ± 0.2	6076.19	3.13 ± 0.20	2.51 ± 0.40
$(1/2^-)$	9869.7 ± 0.8	6087.44	16.0 ± 1.8	1.9 ± 0.9
$(5/2^+)$	9983.0	6207.95	5.0 ± 2.0	109 ± 40

Channel radii: a_n = 3.80 fm, a_α = 6.7 fm

Γ_γ = 2.7 eV for 434 keV resonance, 0.25 eV for other resonances.

E_x = 4143.36 keV + E_R * $A_{O16}/(A_{O16} + A_n)$

* Minus sign means the reduced amplitude product $\gamma_n\gamma_\alpha < 0$.

a. Tilley, et al.[26)] assign $3/2^+$.

b. Tilley, et al.[26)] assign $(5/2^-)$.

1. Individual Resonance Discussion

Selected individual resonances are discussed here. More detailed comments are presented in Ref. 3.

For the 2377.9 keV $s_{1/2}$ resonance, Γ_n and E_R are primarily determined by the high-precision data of Johnson, et al.[8)] corrected for ^{17}O and ^{18}O. The predicted minimum σ_{total}, 0.1013 b, is consistent with the experimental value, 0.1028 ± 0.0018 b. As shown in **Fig. 6**, our evaluation fits the data much better than does ENDF/B-VI.

The 3800-5300 keV region is characterized by several broad overlapping resonances. In companion papers, Johnson[27)] and Fowler, et al.[7)] reported R-matrix analyses leading to J^π assignments and interference patterns for pairs of $p_{1/2}$ and $d_{3/2}$ resonances. Using the more recent Cierjacks data as well as the older data,[4,7,10)] we confirmed the J^π assignments and interference signs of Johnson. For example, for the 3990-4312 keV $p_{1/2}$ pair and the 4180-5066 keV $d_{3/2}$ pair, the sign of $\gamma_n\gamma_\alpha$ must be negative to fit σ_{total} and $\sigma_{n,\alpha}$.

On the basis of better fits to σ_{total} and $\sigma_{n,\alpha}$, we assign J^π = [$3/2^-$, $9/2^+$] for levels with E_R= [5993, 6076] keV, rather than J^π = [$3/2^+$, $5/2^-$] as given by Tilley, et al.[26)]

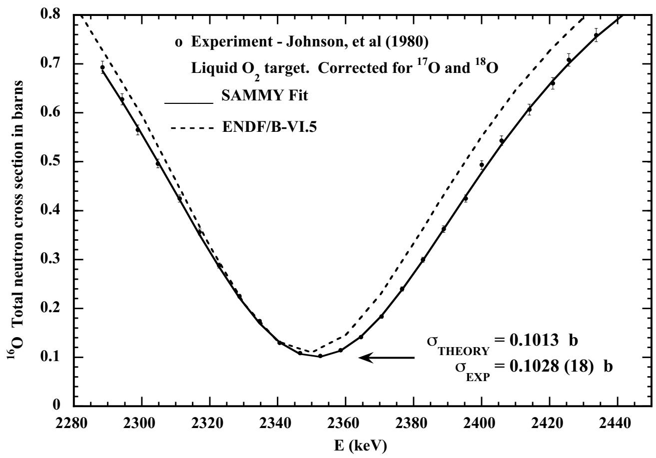

Fig. 6 Comparison of σ_{total} predictions to ENDF/B-VI.5 and data of Johnson et al.[8)]

2. Thermal Cross Sections and Reactor Benchmarks

Free atom total and capture cross sections for E_n = 0.0253 eV and T = 300K agree with the ENDF/B-VI values:

Cross Section	ENDF/B-VI.5	Present Evaluation	Ratio
Total	4.0138 b	4.0297 b	1.004
Capture	0.190 mb	0.196 mb	1.032

Point-wise cross sections generated from our Reich-Moore resonance parameter representation were used for five thermal reactor benchmarks[28)] consisting of three reflected and two bare spheres of highly enriched uranium as aqueous solutions of uranyl fluoride. These benchmarks are useful for testing fast scattering by H_2O as well as ^{235}U fission and capture in the thermal range. As shown below, our k_{eff} values agree with values based on ENDF/B-VI point-wise cross sections.

Benchmark	ENDF/B-VI.5	Present Evaluation	Δk_{eff}
L-7	1.0006	0.9995	-0.0011
L-8	1.0050	1.0047	-0.0003
L-9	1.0020	1.0021	0.0001
L-10	0.9986	0.9974	-0.0012
L-11	0.9997	0.9996	-0.0001

IV. Summary and Conclusions

We have evaluated ^{16}O neutron cross sections in the resolved resonance region with the multilevel Reich-Moore R-matrix formalism. To give a proper treatment for the α particle exit channel, an algorithm to calculate charged particle penetrabilities and shifts was incorporated into the SAMMY code. Routines based on the CPP algorithm have been integrated into a prototype modification of NJOY. An ENDF format revision will be proposed to accommodate this new feature.

Within uncertainties, theory and experiment are in agreement for σ_{total} , $\sigma_{n,\alpha}$, and $d\sigma/d\Omega$ up to 6.3 MeV. New J^{π} assignments are proposed for levels with E_R = 5993 keV $[3/2^-]$ and 6076 keV $[9/2^+]$. Point-wise cross section values based on our resonance parameter representation have been used for five thermal reactor benchmarks; predicted k_{eff} values are in excellent agreement with values based on ENDF/B-VI point-wise cross sections. Thermal values of σ_{total} and σ_{γ} agree with the corresponding ENDF/B-VI values.

For ^{16}O neutron cross section data, our evaluation gives an accurate, few-parameter representation that should be extremely useful for radiation transport calculations in criticality safety analyses. Since our evaluation fits the 2.35 MeV window data much better than does ENDF/B-VI, it should give more reliable results for applications that are sensitive to σ_{total} in this energy region.

Acknowledgments

We are pleased to acknowledge illuminating discussions with Drs. J. A. Harvey, K. Guber, H. Derrien, D. C. Larson, R. W. Roussin, C. Y. Fu, D. T. Ingersoll, C. Lubitz, and J. C. Nimal. We are indebted to Dr. G. M. Hale for providing us with the 2.35 MeV window data[8)] corrected for ^{17}O and ^{18}O. We thank Dr. M. Jaeger for sending us the (α, n) data of Drotleff, et al.[11)] and Dr. C. Raepsaet for sending us some preliminary comparisons[29)] of different ^{16}O evaluations.

This research was sponsored by the Office of Environmental Management, U.S. Department of Energy, under contract DE-AC05- 00OR227525 with UT-Battelle, LLC.

References

1) G. M. Hale, et al., *Proc. Int. Conf. On Nuclear Data for Science and Technology,* Julich, Germany, 1991.
2) N. M. Larson, ORNL/TM-9179/R5 (2000).
3) R. O. Sayer, ORNL/TM-2000/212 (2000).
4) C. H. Johnson, et al., ORNL-4937 (1974).
5) S. Cierjacks, et al., *Nucl. Inst. Meth.* **169**, 185, (1980).
6) D. C. Larson, et al., Proc. Int. Conf. On Nuclear Cross Sections for Technology, Knoxville, p. 34 (1980).
7) J. L. Fowler, et al., *Phys. Rev.* **C8**, 545 (1973).
8) C. H. Johnson, et al., Proc. Int. Conf. On Nuclear Cross Sections for Technology, Knoxville, p. 807 (1980).
9) M. Ohkubo, private communication to NNDC, BNL (1984).
10) J. K. Bair and F. X. Haas, *Phys. Rev.* **C7**, 1356 (1973).
11) H. W. Drotleff, et al., *Astrophys. J.* **414**, 735 (1993).
12) A. Okazaki, *Phys. Rev.* **99**, 55 (1955).
13) J. L. Fowler and H. O. Cohn, *Phys. Rev.* **109**, 89 (1958).
14) D. D. Phillips, WASH-1028, 29 (1960).
15) J. P. Martin and M. S. Zucker, *Bull. Appl. Phys.* **7**, 72 (1962).
16) W. Hunzinger and P. Huber, *Helv. Phys. Acta.* **35**, 351 (1962).
17) D. Lister and A. Sayres, *Phys. Rev.* **143**, 745 (1966).
18) C. H. Johnson and J. L. Fowler, *Phys. Rev.* **162**, 890 (1967).
19) J. L. Fowler and C. H. Johnson, *Phys. Rev.* **C2**, 124 (1970).
20) W. Kinney and F. G. Perey, ORNL-4780 (1972).
21) L. Drigo, et al., *Nuovo Cimento* **31A**, N.1, 1 (1976).
22) A. R. Barnett, *Comp. Phys. Comm.* **27**, 147 (1982); *Comp. Phys. Comm.* **21**, 297 (1981).
23) R. E. MacFarlane and D. W. Muir, LA-12740-M (1994).
24) N. M. Greene, et al., ORNL/CSD/TM-283 (1992).
25) E. Caro, *Proc. Intl. Conf. On the Physics of Nucl. Science and Technology*, Long Island, N. Y., (1998).
26) D. R. Tilley, et al., *Nucl. Phys.* **A564**, 1 (1993).
27) C. H. Johnson, *Phys. Rev.* **C7**, 561 (1973).
28) J. K. Fox, et al., ORNL-2609, 42 (1958).
29) C. Raepsaet, CEA SERMA/LEPP/RT/00-2738/A (2000).